Some Successes and Challenges in Percutaneous Interventions

Gabor Fichtinger, PhD

Director of Engineering,
Associate Research Professor of Computer Science, Mechanical Engineering, and Radiology

GaborF@jhu.edu

Center for Computer-Integrated Surgical Systems and Technology,
Johns Hopkins University

Outline

- **MRI guided prostate interventions**
- **Ultrasound guided liver ablation**

Transrectal Prostate Intervention Robot in Closed MRI Scanner

G Fichtinger[1], A Krieger[1], I Iordachita[1], E Atalar[2],LL Whitcomb[1] , P Guion[3], A Singh[3], C Menard[4], J Coleman[5]

1 The Johns Hopkins University, Baltimore
2 Bilkent University, Ankara, Turkey
3 National Institutes of Health, Bethesda
4 Princess Margaret Hospital, Toronto, CA
5 Memorial Sloan Kettering Cancer Center, New York

Funding
NIH 1R01EB002963, NSF EEC 9731478

Motivation – Prostate Caner

- Over 1 Million prostate biopsies
- 230,000 new cases (annually in the U.S. alone)
- Will double by 2025

The MRI promise:

- Excellent sensitivity in detecting prostatic tissue abnormalities
- Ability of morphological, functional and molecular imaging
- May allow for 'targeted biopsy"

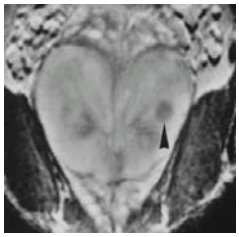

Our Approach – Robotic Assistant in Conventional MRI Scanner

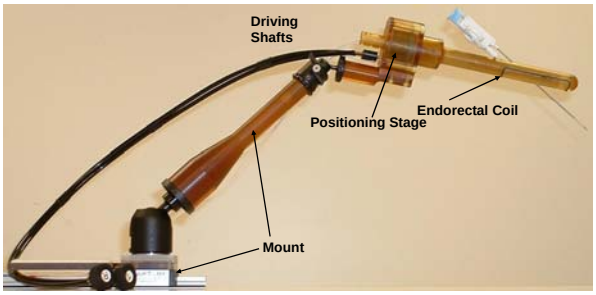

- A. Krieger, R. Susil, C. Menard, J. Coleman, G. Fichtinger, E. Atalar, L. Whitcomb. Design of A Novel MRI Compatible Manipulator for Image Guided Prostate Interventions. IEEE Transactions on Biomedical Engineering, February 2005.

Our Approach – Robotic Assistant in Conventional MRI Scanner

37 patients treated

- Ménard et al. An Interventional MRI Technique for the Molecular Characterization of Intra-Prostatic Dynamic Contrast Enhancement. Molecular Imaging, January-March 2005, 4(1): 63-66
- Susil et al., Transrectal Prostate Biopsy and Fiducial Marker Placement in a Standard 1.5T MRI Scanner, J Urol. 2006 Jan;175(1):113-20.

Biopsy Example

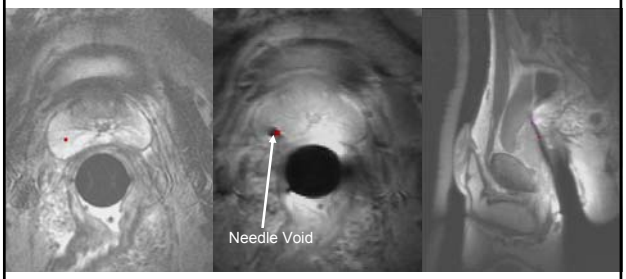

MR images during a clinical procedure:
Left: A target (red dot) is selected on an axial TSE T2-weighted image.
Middle: The needle tip void is visualized in an axial TSE Proton Density image. The desired target matches the actual position of the needle.
Right: The needle void is visualized on a sagittal TSE Proton Density image, where the estimated needle path (red and purple dots) matches the actual path.

Occasional Imaging Artifacts

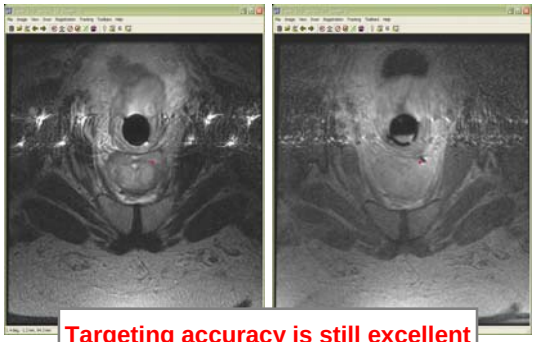

Targeting accuracy is still excellent

Real-time Tracking w/ Active Micro-coils

PROS

- High accuracy (0.2 mm and 0.3 degrees)
- High speed (20 Hz)
- Direct real-time tracking of the surgical tool (needle)

Real-time Tracking w/ Active Micro-coils

CONS

- Custom tracking pulse sequence and data interface
- Occupies 3 channels (limits number of simultaneous imaging coils)
- Custom electronics is prone to failure (4 cases aborted)

New Objectives

- Independence from scanner
- Cheaply replicable
- No engineering support
- No custom electronics
- No pre-calibration
- Reduced imaging artifacts

New Kinematics, Mechanics, and Mount

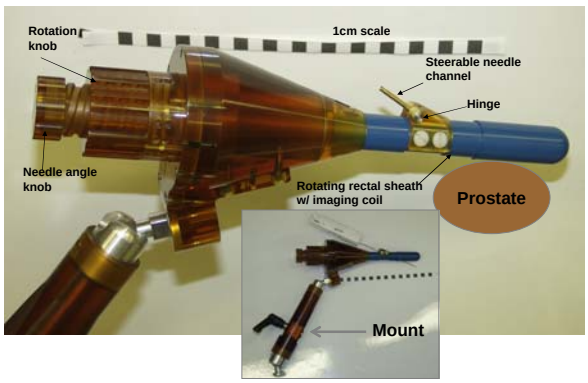

6-DOF Hybrid Tracking

Homing: passive fiducials for absolute location of each robot joint
Incremental Motion: real-time incremental encoding of each joint

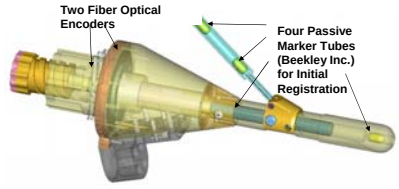

A Krieger, I Iordachita, G Metzger, P Guion, E Atalar, G Fichtinger, LL Whitcomb, Accuracy of Hybrid Tracking for a Novel MR-Guided Transrectal Prostate Interventional Device, 6th Interventional MRI Symposium, Leipzig, pp 143-145, 2006

6-DOF Hybrid Tracking – Cheap Optical Joint Encoders (Rotation)

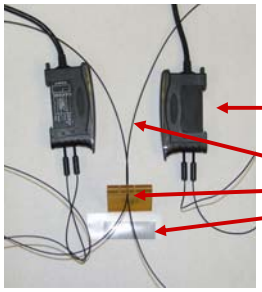

- Banner fiber optic sensors (outside the scan room)
- 0.25 mm plastic fiber in opposing style
- 2 channel quadrature setup
- Resolution of 0.125 mm.

6-DOF Hybrid Tracking – Cheap Optical Joint Encoders (Translation)

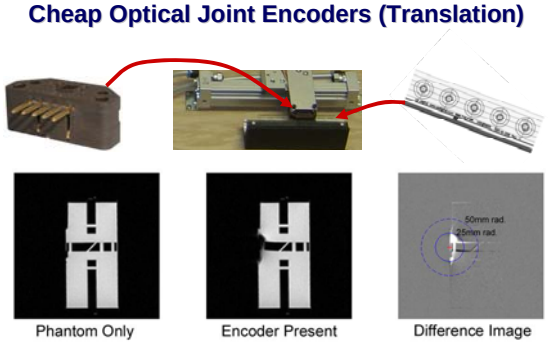

Negligible imaging artifact at 50mm from isocenter (at 1.5T)

Hybrid Tracking Error w/ New Robot

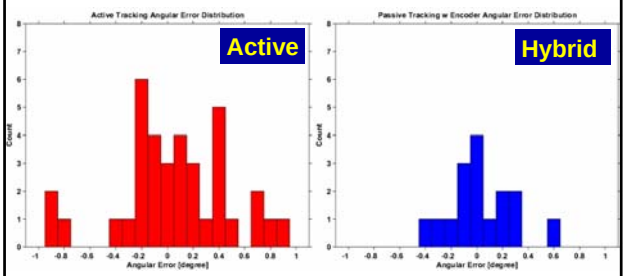

A Krieger, I Iordachita, G Metzger, P Guion, E Atalar, G Fichtinger, LL Whitcomb, Accuracy of Hybrid Tracking for a Novel MR-Guided Transrectal Prostate Interventional Device, 6th Interventional MRI Symposium, Leipzig, pp 143-145, 2006

Summary of Recent Progress

- New robot & tracking scheme developed
- Errors compare favorably to existing methods
- Uses standard MRI pulse sequences
- Does not occupy any receiver channels
- Full MR compatibility
- Ease of deployment on different scanners
- FDA & IRB approvals obtained for trials
- Clinical trials at NIH in November, 2006
- System shipped to Princess Margaret Hospital

Disclosures & Acknowledgments

Disclosures
none

Funding
NIH 1R01EB002963, NSF EEC 9731478

Collaborators

NCI
- Robert Grubb
- Ahmed Gharib
- David Thomasson
- Karen Ullman
- Peter Choyke

Johns Hopkins
- Robert Susil
- Csaba Csoma
- Siddharth Vikal
- Abdel-Monem El-Sharkawy
- Di Qian

Ultrasound Monitoring of Tissue Ablation

Emad Boctor[1], M. deOliveira[2], M. Choti[2], R. Ghanem[1], R. Taylor[1], G. Hager[1], G. Fichtinger[1]

[1] Engineering Research Center (CISST ERC)
[2] Department of Surgery
Johns Hopkins University

Funding
NSF EEC 9731478, Siemens Corporate Research

Thermal Ablation of Liver Tumors

- 1M /year liver cancers worldwide
- The most frequent hepatic malignancy
- Surgical resection is the first choice
- Mixed treatments: un-resectable liver tumors ablated under ultrasound guidance in the same open surgery

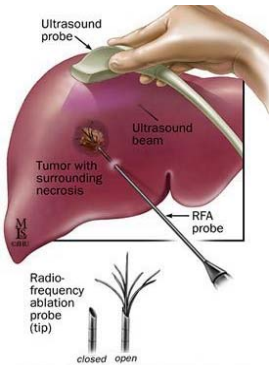

Hopkins dual arm testbed

Testbed for calibration, control, and interventions

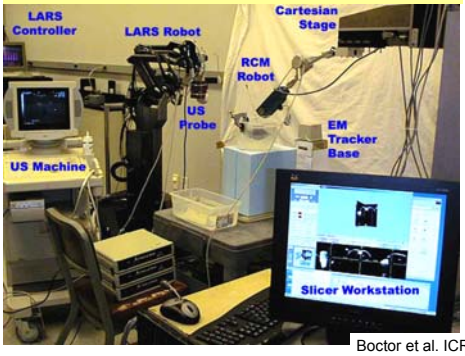

Boctor et al. ICRA 2004

In-Vivo Pig Experiment (2005)

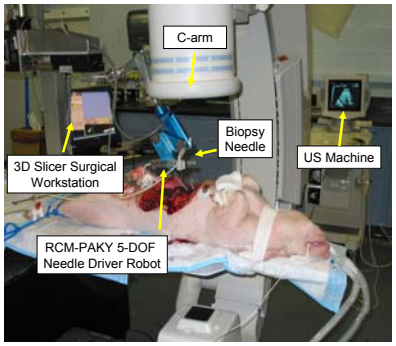

Boctor et al. CARS 2005

Ablation under US Guidance is Blind

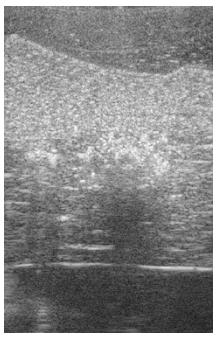

B-mode image

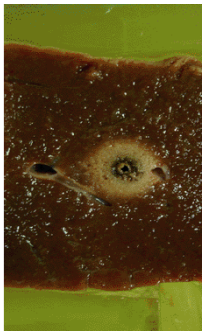

Gross-pathology

Changes of Stiffness – Strain Imaging

(Pioneered by Ophir, Bamber, Varghese, etc.)

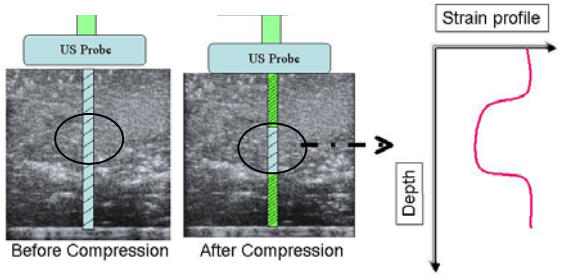

Before compression: Particles with uniform spacing
After compression: Two groups of particle spacing
Differentiate axial displacement to yield axial strain (per continuum mechanics)
Small spacing (green) → soft tissues moved more → high strain
Large spacing (blue) → hard tissues move less → low strain

Limits of Conventional Strain Imaging

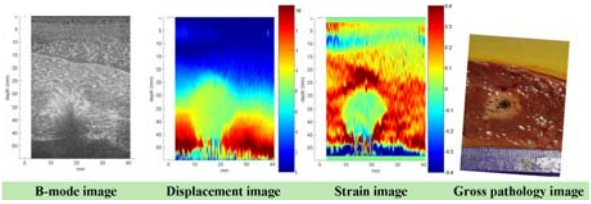

- Strain image can only approximate the ablated lesion
- Dynamic changes of tissue (gassing, charring, etc.) → aggressive changes in attenuation, shadowing, etc.
- Noisy US signal → Decorrelation noise → bad Displacement image
- Displacement to Strain least square differentiator amplifies the noise
- Hard to estimate Young's modulus from strain alone (stress is not uniform under the probe)
- 2D only
- Tends to be inconsistent even under extreme care

Elasticity-based Segmentation

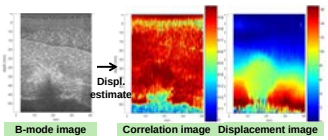

Boctor et al. MICCAI 2005

Elasticity-based Segmentation

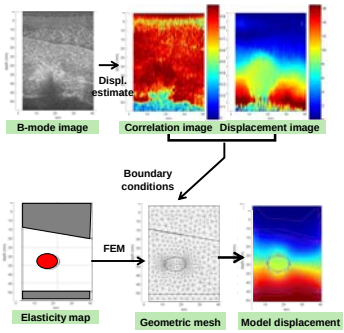

$$\rho\frac{\partial^2 u}{\partial t^2} - \nabla \bullet c\nabla u = K$$

Navier's equation

Boctor et al. MICCAI 2005

Elasticity-based Segmentation

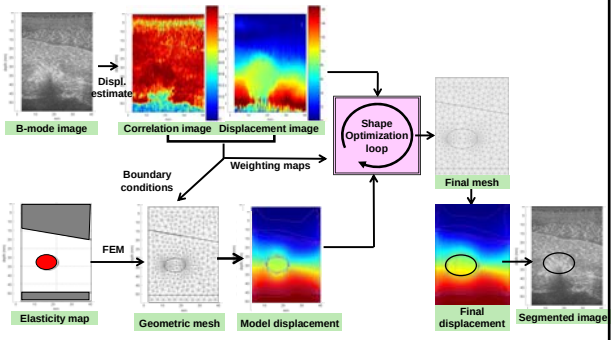

$$\hat{S} = \arg\min\{\Im(S) = \sum_{i=1}^{N}\sum_{j=1}^{M} W(i,j)\left\|\tilde{u}(i,j) - u(i,j;S)\right\|^{L1}\}$$

Boctor et al. MICCAI 2005

Segmentation Example

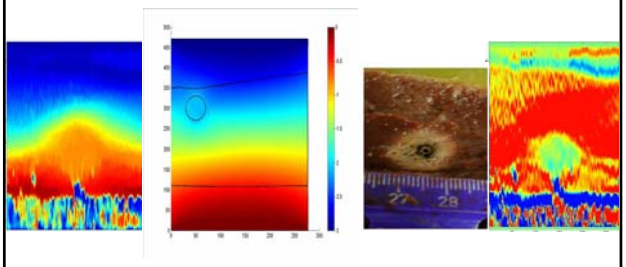

True Displacement | Model Displacement | Pathology | Strain Image

Boctor et al. MICCAI 2005

Convergence Results

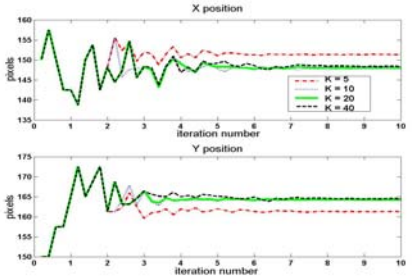

- Convergence error is within a few pixels
- K is the ratio of Young's modulus of cooked and normal liver
- 20 (**green curve**) is the correct value (literature & our own measurement)
- Robust to large errors in estimating K (between about 10 & 40)

Boctor et al. MICCAI 2005

Overlapping Tumors & Burns

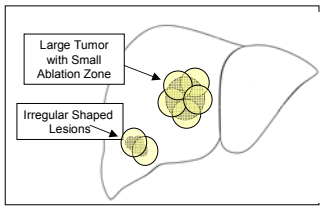

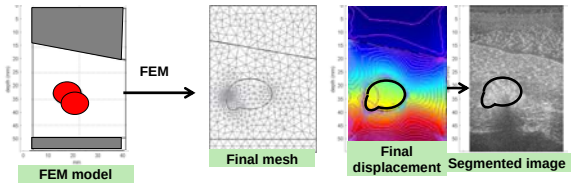

Boctor et al. MICCAI 2005

3D Segmentation

Series of 2D FEM models

Solid 3D FEM model

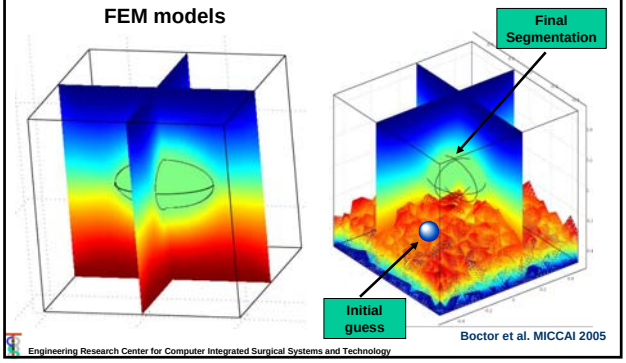

Boctor et al. MICCAI 2005

Ultrasound Speckle Detection

- Each pixel is formed by the back scattered echoes from an approximately ellipsoid called the resolution cell.
- Such a summation of backscatters results in a granular image.
- Although of random appearance, speckle pattern is identical if the same object is scanned under the same focusing, frequency and direction.
- If each resolution cell has a number of scatterers more than 10 which are placed uniformly, a fully developed speckle is formed by definition.

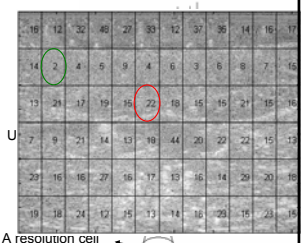

A resolution cell

Bovine liver

- Using $R=\frac{\langle A\rangle}{\sigma}$ and $S=\frac{\left\langle\left(A-\langle A\rangle\right)^3\right\rangle}{\sigma^3}$

where $\sigma^2=\langle A^2\rangle-\langle A\rangle^2$, a patch with large number of pixels can be classified.

Rivaz et al. IEEE US Symposium, Vancouver, 2006

Ultrasound Speckle Detection

$$R=\frac{\langle A^{vR}\rangle}{\sigma_{vR}} \quad S=\frac{\left\langle\left(A^{vS}-\langle A^{vS}\rangle\right)^3\right\rangle}{\sigma_{vS}{}^3} \quad \sigma_v{}^2=\langle A^{2v}\rangle-\langle A^v\rangle^2$$

Data A is obtained in simulation by summing μ vectors (no. of scatterers) of length √(2/ μ), i.e. random walk, and a vector of length k (coherency)

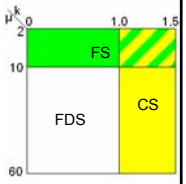

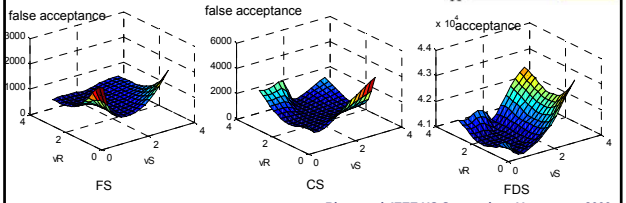

Rivaz et al. IEEE US Symposium, Vancouver, 2006

Ultrasound Calibration

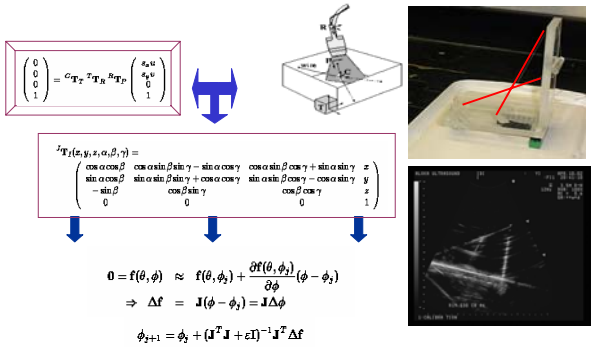

$$\mathbf{0}=\mathbf{f}(\theta,\phi) \approx \mathbf{f}(\theta,\phi_2)+\frac{\partial \mathbf{f}(\theta,\phi_2)}{\partial\phi}(\phi-\phi_2)$$

$$\Rightarrow \Delta\mathbf{f} = \mathbf{J}(\phi-\phi_2)=\mathbf{J}\Delta\phi$$

$$\phi_{i+1}=\phi_2+(\mathbf{J}^T\mathbf{J}+\varepsilon\mathbf{I})^{-1}\mathbf{J}^T\Delta\mathbf{f}$$

- Prager RW, Rohling RN, Gee AH, Berman L. Rapid Calibration for 3-D Freehand Ultrasound, *US in Med. Biol.*, 24(6):855-869, 1998
- Mercier L, Lango T, Lindseth F, Collins DL. A review of calibration techniques for free-hand 3-D ultrasound systems. Ultrasound Med Biol, 2005;31(4):449-471.

Conventional Workflow

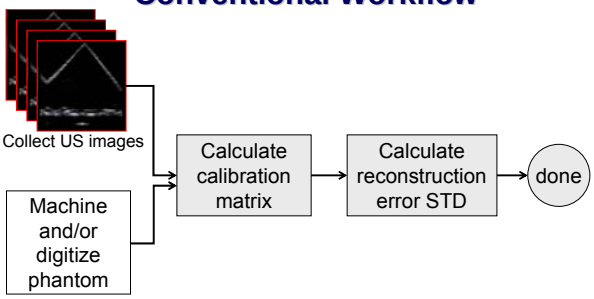

Linear pipeline → residual error
- **Needs large number of images**
- **Slow non-linear optimization**

Bootstrapped Calibration

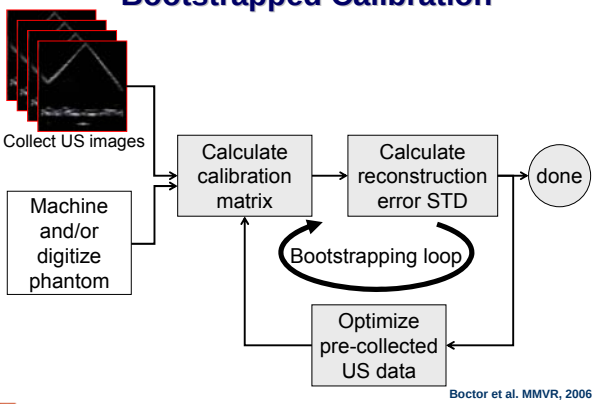

Boctor et al. MMVR, 2006

AX=XB Closed Formulation

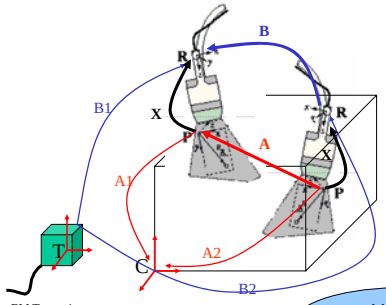

$$B = B_2^{-1} B_1$$

$$A = A_2 A_1^{-1}$$

$$AX = XB$$

How to estimate *A*?

Real-time evaluation
3 US images enough ☺

Boctor et al. IEEE-ISBI, 2004

Patient Specific In-Vivo Self-calibration

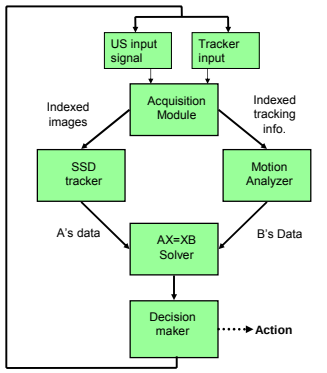

Convergence under different image tracking steps

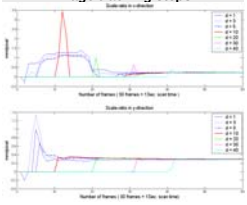

Calibration achieved with 10-20 steps, 0.3-0.6 sec scanning time, and 1.5 mm probe travel

Boctor et al. MICCAI 2005

Disclosures & Acknowledgments

Disclosures
none

Funding
NSF EEC 9731478, Siemens Corporate Research

Thank you !